Photophysics of New Water-Soluble Terrylenediimide Derivatives and Applications in Biology

Christophe Jung,[a] Nadia Ruthardt,[a] Robert Lewis,[a] Jens Michaelis,[a] Beate Sodeik,[b] Fabian Nolde,[c] Kalina Peneva,[c] Klaus Müllen,[c] and Christoph Bräuchle*[a]

The photophysical properties of three new water-soluble terrylenediimide (WS-TDI) derivatives are investigated and their utilization in biological experiments is demonstrated. Each of these dyes can be excited in the far red region of the visible spectrum, making them good candidates for in-vivo studies. Single-molecule techniques characterize their photophysics that is, the number of emitted photons, blinking characteristics and survival times until photobleaching takes place. All three dyes exhibit bright fluorescence, as well as an extremely high resistance against photodegradation compared to other well-known fluorophores. Due to their different characteristics the three new WS-TDI derivatives are suitable for specialized biological applications. WS-TDI dodecyl forms non-fluorescent aggregates in water which can be disrupted in a hydrophobic environment leading to a monomeric fluorescent form. Due to its high lipophilicity WS-TDI dodecyl anchors efficiently in lipid bilayers with its alkyl chain and hence can be ideally used to image membranes and membrane-containing compartments in living cells. In contrast, the positively charged WS-TDI pyridoxy is a new type of chromophore in the WS-TDI family. It is fully solubilized in water forming fluorescent monomers and is successfully used to label the envelope of herpes simplex viruses. Finally, it is shown that a WS-TDI derivative functionalized with N-hydroxysuccinimide ester moiety (WS-TDI/NHS ester) provides a versatile reactive dye molecule for the specific labelling of amino groups in biomolecules such as DNA.

1. Introduction

The use of fluorescent labels has facilitated and advanced the investigation of complex biological processes. Over the last years a large variety of labelling strategies has been developed allowing the visualisation of different biological systems like proteins and cellular compartments using fluorescence microscopy. Moreover, the exact localisation of labelled single particles can be monitored in real time using fluorescence microscopy in living cells, revealing the dynamics of biological molecules such as proteins, viruses or lipids.[1,2] Hence, single-molecule spectroscopy (SMS) has become a common method to study the dynamical behaviour of biomolecules with the advantage of suppressing ensemble averaging.[3,4] It is now possible to measure dynamic processes such as protein–protein interactions[5], or to monitor the mobility of single motor proteins.[6–10] While most of these processes so far have been investigated in vitro, novel experimental developments allow life-cell investigation.[11,12] Through such SMS measurements it is clear that, in order to observe the label for a longer period of time, the fluorophores must exhibit a bright fluorescence signal, or in other words, show a high quantum yield and a large absorption coefficient. Additionally, a useful fluorophore should exhibit a high resistance against photobleaching thereby increasing the observation time and the amount of collectable data. For example, the observation of single particles during the complete cell cycle can require observation times of several hours. Moreover, for applications in biology the dye molecules must show a good solubility in water and their fluorescence spectrum should lie in the far red region of the visible range in order to limit the autofluorescent background in living cells.

Hence, the need for new water-soluble fluorescent labels has rapidly expanded within the last decade. Terrylenediimide (TDI) dye molecules are among the most promising candidates to fulfill these requirements because they exhibit bright, red-shifted fluorescence and show high chemical stability.[13] Moreover, their photostability that is, the resistance against photodegradation is dramatically higher than those of other available fluorophores, which is a crucial advantage for long term sensitive fluorescence applications. We have recently reported on the characterization of a new water-soluble terrylenediimide (WS-TDI, structure shown in Figure 1a), and its utilization in biological experiments.[14] This dye molecule is obtained by

[a] Dr. C. Jung, Dr. N. Ruthardt, R. Lewis, Prof. Dr. J. Michaelis,
Prof. Dr. C. Bräuchle
Department of Chemistry und Biochemistry and Center for Nanoscience (CeNS)
Ludwig-Maximilians-Universität München
Butenandtstrasse 11, 81377 München (Germany)
Fax: (+49) 89 2180 77548
E-mail: Christoph.Bräuchle@cup.uni-muenchen.de

[b] Prof. Dr. B. Sodeik
Institute of Virology, Hannover Medical School
Carl-Neuberg-Str. 1, 30625 Hannover (Germany)

[c] Dr. F. Nolde, Dr. K. Peneva, Prof. Dr. K. Müllen
Max Planck Institute for Polymer Research
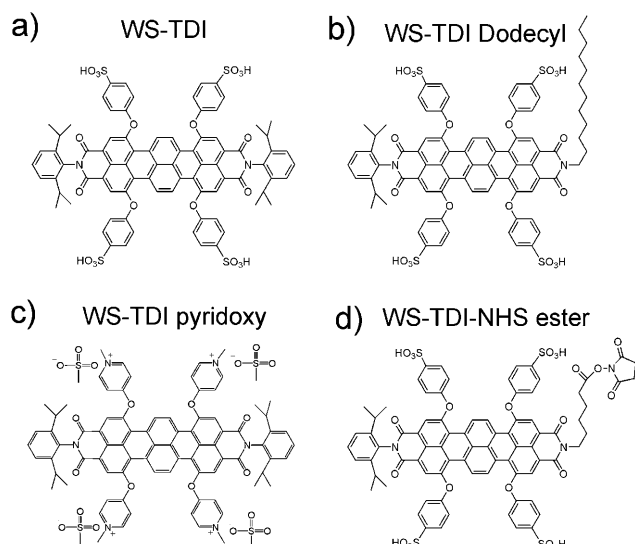Ackermannweg 10, 55128 Mainz (Germany)

Figure 1. Structure of the WS-TDI derivatives. a) WS-TDI. b) WS-TDI dodecyl. c) WS-TDI pyridoxy. d) WS-TDI/NHS.

combining the hydrophobic terrylene core with four anionic sulfonyl side groups to provide solubility in aqueous media.[15] This strategy leads to a highly photostable fluorophore which forms soluble aggregates in water. The fluorescence of WS-TDI is quenched in the aggregates. However, due to their high lipophilicity, the WS-TDI molecules form strongly fluorescent monomers in lipophilic environments. These properties make WS-TDI a very interesting dye molecule for the labelling of membranes and membrane containing compartments in living cells. Here we report on the photophysical characterization and biological applications of three new WS-TDI molecules which are derived from the initial structure of WS-TDI offering new, specific functionalities.

Labelling cell membranes is difficult since the small thickness of a lipid bilayer (typically in the order of 2–3 nm) limits the maximum uptake of dye molecules. The labelling efficiency of WS-TDI in such membranes can be improved by strengthening the interactions between the dye molecules and the membrane lipid bilayer. This can be achieved by introducing a dodecyl alkyl chain in the WS-TDI molecule as done in WS-TDI dodecyl (structure shown in Figure 1b). The long alkyl chain acts as an anchor in the lipid bilayer and the new compound is expected to be more lipophilic than WS-TDI, and, as a consequence, can penetrate more efficiently into cell membranes.

A strong demand for a larger variety of applications asks for a WS-TDI derivative forming water-soluble fluorescent monomers. A further property of WS-TDI which can be modified is the polarity of the fluorophore. WS-TDI and WS-TDI dodecyl each have four negative charges located on the sulfonyl side groups. Using positively charged pyridoxy substituents in the bay region (WS-TDI pyridoxy, see Figure 1c) we developed a corresponding positively charged WS-TDI derivative. Especially interesting is the influence of the positive charges on the solubility of this molecule in water as well as on its fluorescent properties.

Finally, it is highly desirable to functionalize WS-TDI with a reactive group allowing specific labelling of distinct sites on a target molecule. For instance, the *N*-hydroxysuccinimide ester (NHS-ester) is a functional group which is known for its high affinity for amine groups and is commonly used for the labelling of biological molecules such as proteins, DNA, RNA etc. Such an active group is successfully added to one of the two imide groups of WS-TDI, leading to an active WS-TDI/NHS-ester molecule[16] (see Figure 1d).

It is shown that all compounds have an exceptionally high photostability compared to other commonly used dye molecules. WS-TDI dodecyl penetrates efficiently into lipid bilayers because of its anchor, therefore is ideal for imaging membranes and membrane-containing compartments in living cells. WS-TDI pyridoxy is the first member of the WS-TDI family which is fully solubilized in water forming fluorescent monomers. It is useful in a large variety of applications and as an example we show the successful labelling of the envelopes of herpes simplex type 1 virus particles. Finally, it is shown that WS-TDI/NHS ester provides a versatile active dye molecule for the specific labelling of amino groups in biomolecules such as DNA.

2. Results and Discussion

2.1. Photophysical Parameters of WS-TDI Dodecyl and WS-TDI Pyridoxy

The photophysical parameters of WS-TDI were already described previously.[14] Because of the similarity between the structure of WS-TDI dodecyl and WS-TDI we discuss the comparison of the photophysical properties of these two compounds. The effect of the charge of WS-TDI pyridoxy on the photophysical properties is also discussed. Finally, as WS-TDI/NHS is a molecule specifically designed for being covalently linked to a biomolecule, its photophysics is presented in combination with its application as a DNA-label. An overview of all the photophysical and photostability parameters can be found in Table 1.

Absorption and Fluorescence Spectra

Compared to WS-TDI the alkyl chain in the structure of the WS-TDI dodecyl molecule is expected to have only a weak influence on the terrylene chromophore core, and, as a consequence, on its photophysical properties. The absorption and fluorescence spectra of WS-TDI dodecyl in water are shown in Figure 2a. Both spectra resemble the corresponding spectra of WS-TDI (data not shown)[14]. The absorption spectrum of WS-TDI dodecyl in water (Figure 2a left, black line) shows a broad main band with a maximum at 634 nm and a weak shoulder at 688 nm (for WS-TDI maxima are at 637 nm and 690 nm). Moreover, no fluorescence signal could be detected (Figure 2a, right black line). Additionally, light-scattering measurements are performed for WS-TDI dodecyl (data not shown) and reveal the presence of small particles in water, typically several hundreds of nanometers in size. These observations strongly indi-

Table 1. Photophysical and photostability parameters for the three WS-TDI derivatives and other dyes.

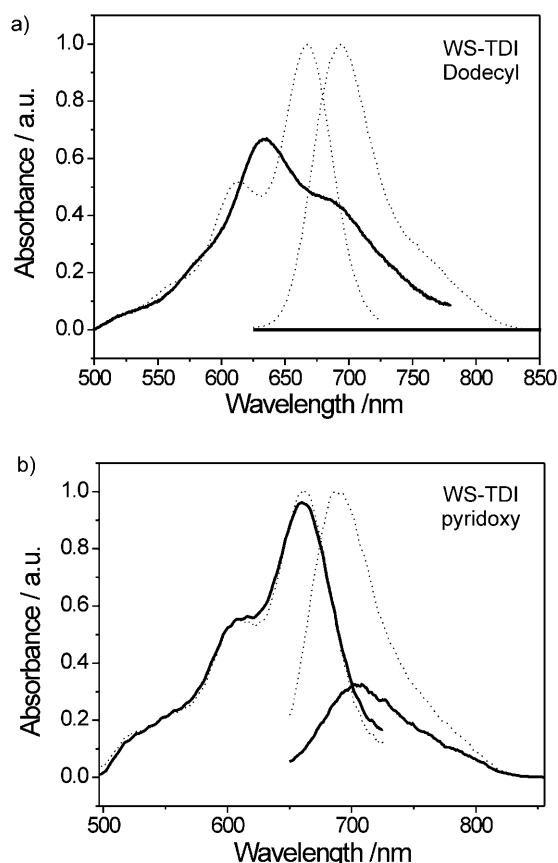| Fluorophore	Water			Water with 10% wt/wt Pluronic			TEP ($\times 10^6$) in PVA	ST [s] in PVA
	λ_{abs}^{max} [nm]	λ_{em}^{max} [nm]	Φ_f	λ_{abs}^{max} [nm]	λ_{em}^{max} [nm]	Φ_f		
WS-TDI	637	–	0	670	700	0.17 ± 0.02	58 ± 5	43 ± 4
WS-TDI dodecyl	634	–	0	666	693	0.14 ± 0.02	43 ± 3	45 ± 10
WS-TDI pyridoxy	660	705	0.016	661	688	0.039 ± 0.003	24 ± 5	30 ± 2
ATTO 647N	644	669	0.65	–	–	–	5 ± 1	1.6 ± 0.1
Cy5	649	670	0.29	–	–	–	3 ± 1	1.7 ± 0.2

Figure 2. Absorption and fluorescence spectra of WS-TDI dodecyl and WS-TDI pyridoxy in water, and in presence of Pluronic P123. a) Absorption and fluorescence spectra of WS-TDI dodecyl in water (——) and in presence of 10% wt/wt of Pluronic (·····). No fluorescence signal is observed in water, whereas the fluorescence is intense in presence of Pluronic. The absorption and emission spectra in presence of Pluronic were not normalized but are scaled accordingly. b) The same for WS-TDI pyridoxy. The fluorophore fluoresces weakly in water.

cate the presence of H-aggregates for WS-TDI dodecyl in water, as already reported for WS-TDI and other fluorophores with large and rigid π-electron systems;[17–20] this phenomenon of aggregation is due to the strong inter-molecular interaction between the hydrophobic dye molecules in polar solvents such as water and is obviously not hindered by the alkyl chain in WS-TDI dodecyl.

The absorption and fluorescence spectra in the presence of 10% wt/wt of Pluronic (Figure 2a doted lines) show a maximum at 666 nm and at 693 nm, respectively. Again, these spec-

tra are very similar to those measured with WS-TDI in the presence of Pluronic (absorption maximum at 670 nm and emission maximum at 700 nm for WS-TDI). The quantum yield in water in the presence of Pluronic for WS-TDI dodecyl and WS-TDI are also similar with $\phi_f = 0.14$ and 0.17, respectively. The onset of fluorescence emission when going from water to a solution of Pluronic can be explained by the disruption of the non-fluorescent dye aggregates and the solvation of the monomers inside the micelles.[14,21]

In the case of WS-TDI pyridoxy we observe a completely different behaviour showing that this molecule forms a new type of chromophore within the family of WS-TDI derivatives. First, the absorption spectrum of WS-TDI pyridoxy in water with a maximum at about 660 nm (see Figure 2b, left, black lines) is not influenced by the presence of 10% wt/wt of Pluronic (Figure 2b, left, dotted line). Moreover, the WS-TDI pyridoxy fluoresces in pure water as well as in water-containing micelles of Pluronic, with emission maxima at 705 nm and 688 nm. Finally, contrary to the two other WS-TDI derivatives no signal was detected in light-scattering measurements of a solution of WS-TDI pyridoxy in water at the same concentration ($C = 10^{-5}$ mol L^{-1}), meaning that no particles that is, no aggregates are present in solution. Altogether these observations suggest that WS-TDI pyridoxy molecules do not form aggregates in water. This is a result of the higher solubility of the WS-TDI pyridoxy molecules in water and is an important difference in comparison to the negatively charged WS-TDI derivatives. Possible reasons for this different behavior may be: 1) bulky pyridoxy groups could prevent interactions of different TDI molecules, 2) the positive charges may be shielded differently, and thus create different repulsion or 3) withdrawing of the electron density from the terrylene core by the pyridoxy groups could weaken intermolecular interactions.

The different solubilities also play a role for the extinction coefficients. The maximum extinction coefficients of WS-TDI pyridoxy in water or in water in the presence of Pluronic are virtually identical [$\varepsilon_{662nm}(H_2O) = 73\,800$ M^{-1}cm^{-1} and $\varepsilon_{662nm}(H_2O, 10\%$ wt/wt Pluronic$) = 77\,100$ M^{-1}cm^{-1}]. In contrast, in the case of WS-TDI a large increase is detected when Pluronic is added [$\varepsilon_{637nm}(H_2O) = 23\,900$ M^{-1}cm^{-1} and $\varepsilon_{670nm}(H_2O, 10\%$ wt/wt Pluronic$) = 42\,000$ M^{-1}cm^{-1}], caused by the disruption of the WS-TDI aggregates in the micelles of Pluronic leading to the fluorescent monomers.[14] We find that in the latter medium, WS-TDI pyridoxy absorbs about two times more than WS-TDI. This stronger absorption is a clear advantage for fluorescence microscopy experiments.

Furthermore, the fluorescence quantum yield of WS-TDI pyridoxy in water is fairly low ($\phi_f = 0.016$). In the presence of 10% wt/wt Pluronic we observe a two-fold increase ($\phi_f = 0.039$). This indicates that a more suitable environment for the fluorophore is in the hydrophobic inner part of the micelles, since it is known that the quantum yield of a fluorophore is very sensitive to its environment.[22, 23] This value is, however, lower than the quantum yield of WS-TDI and WS-TDI dodecyl and limits to some extends the brightness of this dye. The brightness depends on the product of extinction coefficient and quantum yield.

In summary the absorption and fluorescence properties of WS-TDI and WS-TDI dodecyl are very similar, indicating that the dodecyl chain has a very weak influence on the chromophore. In contrast, the pyridoxy groups of WS-TDI pyridoxy allow an increased solubility in water without the formation of aggregates, and WS-TDI pyridoxy is the first dye within the WS-TDI family which fluoresces in water. Theoretical calculations have to be performed to give a conclusive explanation for these differences which seem to be caused by the negatively charged sulfonyl groups and the positively charged pyridoxy groups. Modelling of weak interactions such as π-stacking in the presence of solvent molecules like water is difficult to perform and thus beyond the scope of this work.

Photostability

Apart from the described absorption and fluorescence properties, evaluating the capabilities of dyes for single-molecule applications requires testing at the single-molecule level and determining the number of emitted photons and the survival times before photobleaching. The photostability of the three water-soluble terrylene derivatives is measured and compared to ATTO647N and Cy5, which are two fluorophores with similar absorption and fluorescence spectra, known for their high photostability and commonly used in biological studies. One way to investigate single molecules is to immobilize them by spin-coating a highly diluted polymer solution as a thin film on a substrate. Under these conditions, the molecules are so widely separated that on average less than one molecule is in the confocal spot of the laser beam. Scanning the laser beam across the sample allows single molecules to be detected by their fluorescence (see the Experimental Section). The fluorescence of individual molecules is observed by positioning the laser beam on such a spot and collecting the emitted fluorescence as a function of time. A typical fluorescence intensity trajectory for a single WS-TDI dodecyl molecule is shown in Figure 3a. This trajectory shows blinking events at about 20 s and 24 s as well as one-step photobleaching at about 27 s. The digital on–off switching of the fluorescence intensity is a typical signature for a single molecule. From such a fluorescence intensity trajectory, the number of total emitted photons (TEP) can be extracted by computing the integral over time and correcting for the detection efficiency of the setup (see Experimental Section). Moreover, the survival time (ST) that is, the time until irreversible photobleaching occurs can be obtained.
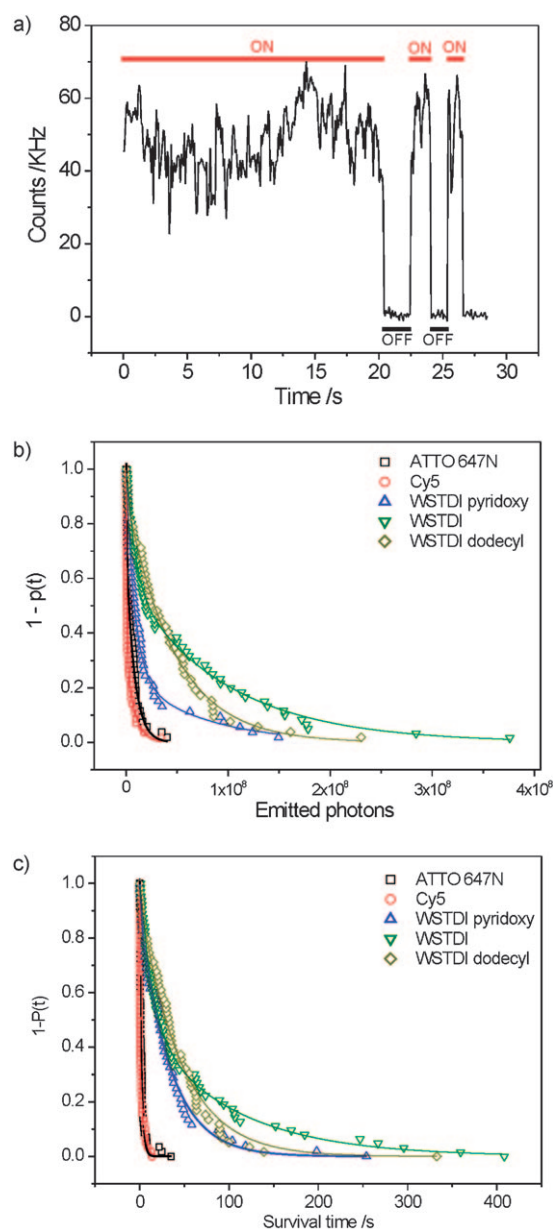

Figure 3. Photostability measurements. a) A typical fluorescence intensity trajectory for WS-TDI dodecyl. The molecule exhibits blinking behavior and undergoes irreversible photobleaching. The ON and OFF periods are overlayed as black and red stripes. b) Accumulated probability distributions of the TEP for WS-TDI, WSTDI dodecyl, WS-TDI pyridoxy, Cy5, and ATTO 647N. Similarly to the study of WS-TDI[14] the curves cannot be fitted with a single exponential decay. Instead, two-component decays are used (solid lines), from which we calculated average TEPs. c) Similar evaluation for the ST with bi-exponential fits shown as solid lines.

The distributions of these two parameters characterize the capabilities of the fluorophores for single-molecule applications.

The dye molecules are embedded at ultra-low concentration ($C \sim 10^{-9}$ mol L^{-1}) in poly(vinyl alcohol) (PVA) polymer films. Figures 3b and c show the probability distributions of the TEP and the ST extracted from intensity time trajectories. About 60 single molecules of each fluorophore are measured under comparable experimental conditions. For WS-TDI in PVA the average TEP is $(58 \pm 5) \times 10^6$, and the average ST is 43 ± 4 s. For

WS-TDI dodecyl in PVA the TEP = $(43\pm3)\times10^6$ and ST = 45 ± 10 s. When one compares the slightly lower value of the quantum yield of WS-TDI dodecyl ($\phi_f = 0.14\pm0.02$) to WS-TDI ($\phi_f = 0.17\pm0.02$) one can explain that less photons are emitted by WS-TDI dodecyl before photobleaching. However, the survival times of both dyes are very similar, indicating that the presence of the alkyl chain has a limited influence on the photostability of the fluorophore. In contrast, WS-TDI pyridoxy has an average TEP of $(24\pm5)\times10^6$ and an average ST of 30 ± 2 s. It emits more than two times less photons than WS-TDI in PVA, and photobleaches about 30% faster. Apparently, the pyridoxy groups change the quantum yield and the photobleaching behaviour. Nevertheless, all three water-soluble terrylene derivatives emit over five times more photons before photobleaching, and live more than 18 times longer than ATTO647N or Cy5, demonstrating that these novel water-soluble terrylene derivatives have much higher photostability. Noteworthy is that all these measurements were conducted in a polymer matrix, and not in aqueous solutions in which properties of the dyes (such as photostability, quantum yield etc.) may vary and that the relatively high polarity of PVA ($\varepsilon = 5$) makes it a suitable environment for comparison with water.

In summary, the outstanding photostability of the new WS-TDI dyes makes them very promising candidates for ensemble as well as for single-molecule experiments. Some of these experiments have been performed in order to illustrate interesting areas for application of these dyes.

2.2. Membrane Labelling

Fluorescence Spectra in Living Cells

As mentioned above, WS-TDI dodecyl is expected to incorporate more efficiently into lipid membranes than WS-TDI because of the presence of its lipophilic alkyl chain. We test this assumption by monitoring the dye uptake into living cells by fluorescence spectroscopy.

The fluorescence emission spectra of WS-TDI and WS-TDI dodecyl in a PBS solution at a concentration of 10^{-5} mol L^{-1} are displayed in Figure 4 (dotted black and grey lines, respectively). In both cases no fluorescence signal is detected (only in-
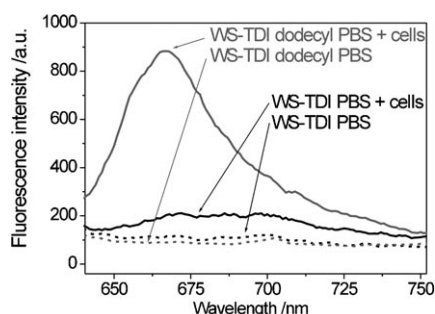

Figure 4. Fluorescence spectra of WS-TDI and WS-TDI dodecyl in PBS, and in PBS in presence of living HeLa cells. The fluorescence intensity measurements with the living cells show that for the WS-TDI dodecyl dye the fluorescence intensity is five-times stronger than for the WS-TDI dye.

strument background) since the dye molecules are sequestered in non fluorescing aggregates in water. The black and grey lines show the fluorescence spectra of solutions of WS-TDI and WS-TDI dodecyl in the presence of HeLa cells (cell density = 10^6 cells mL^{-1}), one hour after addition of the dye. For both dyes the appearance of a fluorescence signal with a maximal intensity at around 670 nm is observed. This can be explained by the disruption of the dye aggregates and the solvation of fluorescing monomers in membranes and membrane-containing compartments of the living cells. By integrating the fluorescence spectra we find a five-times stronger fluorescence intensity of WS-TDI dodecyl compared to WS-TDI in the presence of the same amount of cells. This indicates that the dye-uptake process is more efficient for WS-TDI dodecyl; the hydrophobic chain greatly helps in the incorporation of the fluorophore into the lipid membrane, as was expected from the more lipophilic nature of the WS-TDI dodecyl molecule.

Life Cell Imaging

The high affinity of the WS-TDI derivatives for lipid environments can be used to image membranes of living cells. Living HeLa cells growing on chambered cover glass were incubated with a medium containing 10^{-5} mol L^{-1} WS-TDI, WS-TDI dodecyl, and WS-TDI pyridoxy, respectively, at 37 °C. After one hour, the cells were washed three times with PBS in order to remove excess dye, and were subsequently imaged. The fluorescence light of the three dyes was detected with the standard detector (photomultiplier) of a confocal laser scanning microscope, as shown in Figures 5 a–c. The corresponding transmission images which show the cell shapes are depicted in Figures 5 d–f. Figure 5 a shows a confocal section of living HeLa cells stained with WS-TDI. In each cell, numerous endosomal vesicles appear as bright spots. The cell membrane is hardly visible, indicating that the loosely bound dye in the plasma membrane had been washed out whereas intracellular dye in the vesicles remained. Figure 5 b shows a fluorescence image for WS-TDI dodecyl. Similarly to WS-TDI, endocytic vesicles are labelled, but in addition also labelling of the cell membrane is detectable. The residual membrane labelling after the washing steps demonstrates that the long alkyl chain of WS-TDI dodecyl anchors the dye molecules more efficiently to the lipid bilayer membrane as compared to WS-TDI. The labelling pattern of the charged WS-TDI pyridoxy is comparable to WS-TDI as presented in Figure 5 c. However, the endosomes labelled with WS-TDI pyridoxy appear with a brighter fluorescence signal. The reason for this seems to be the higher number of monomer dye molecules which are available in the PBS solution due to the higher solubility of WS-TDI pyridoxy.

The pathway of endosomes labelled with the new fluorophores can be monitored by wide-field microscopy. Four sequences of fluorescence images [600 frames, 500 ms/frame, (20 µm × 20 µm in size) measured under the same experimental conditions] of HeLa cells stained with either WS-TDI, WS-TDI dodecyl, WS-TDI pyridoxy, or Alexa647/dextran [the concentration of the fluorophore before washing was C ~ 10^{-6} mol L^{-1} in all cases] are shown in the Supporting Information (Movie 1).
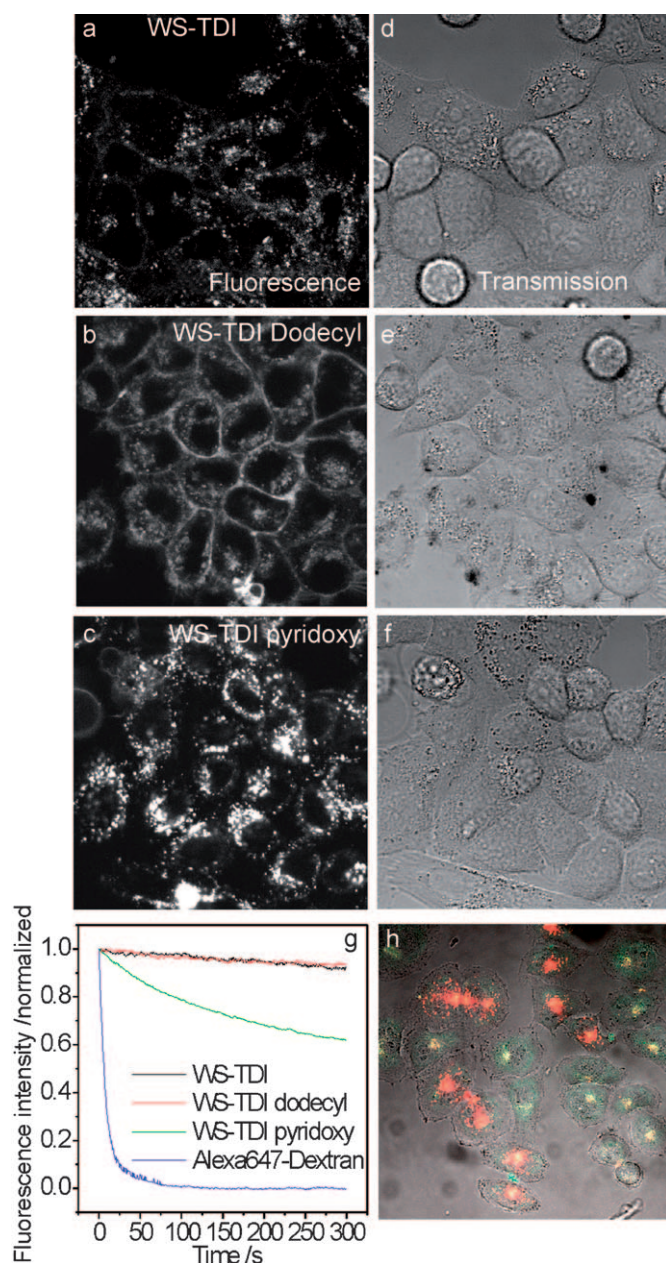
Figure 5. Life cell imaging with WS-TDI derivatives. Confocal fluorescence images of living HeLa cells stained with a) WS-TDI, b) WS-TDI dodecyl, and c) WS-TDI pyridoxy after washing. The cells show prominent labelling of endocytic vesicles. In the case of WS-TDI dodecyl, residual dye remained in the plasma membrane. d–f) Corresponding transmission light images. g) Plot of the normalized fluorescence intensity as a function of time of HeLa cells adhered onto a cover glass in PBS and stained with WS-TDI, WS-TDI dodecyl, WS-TDI pyridoxy, and Alexa647/dextran. The plot corresponds to the data from Movie 1 in the Supporting Information. h) Overlay of a transmission light image with a confocal section of dye-labelled HeLa cells mixed with unlabelled cells. WS-TDI (red signal) propagates to daughter cells during cell division as indicated by the adjacent labelled cell doublets and does not show toxic long-term effects. The yellowish-green signal represents the unspecific autofluorescence of unlabelled cells.

Alexa647/dextran is a well-known fluid phase marker and is used as a reference to evaluate the capability of the three new terrylene derivatives used as markers for the endosomic traffic, and to compare their photostability.

In each of the four movies the movement of the endosomes can be monitored in real time, which demonstrates that the three new fluorophores can be used for marking the membrane-containing compartments of living cells. Let us note that the signal-to-noise ratio, which is relevant, for example, for high positioning accuracy,[24,25] is higher for WS-TDI and WS-TDI dodecyl compared to the two other dyes. This is due to the fact that these two dyes form non-fluorescent aggregates in water solution, and thus do not contribute to a general fluorescence background. The most important parameter, however, is the decay of the fluorescence intensity with time. This is displayed in Figure 5d for the four investigated fluorophores. Whereas the fluorescence intensity of the Alexa647/dextran (blue line) decays rapidly to nearly zero within some seconds (with the high intensity of $0.2 \, \text{kW cm}^{-2}$ used in this experiment), the signal of WS-TDI (black line) and WS-TDI dodecyl (red line) remains nearly constant during the whole observation time, and the fluorescence intensity of WS-TDI pyridoxy (green line) also fades very slowly. These data agree well with the single-molecule data for the photostability in Figure 3. The extremely high photostability of the three new water-soluble derivatives is thus a major advantage compared with other dyes commonly used in biological studies like Alexa647/dextran.

Long Term Toxicity for Living Cells

To evaluate the long term toxicity of the labelling, WS-TDI labelled HeLa cells are mixed with unlabelled cells (in a ratio of labelled cells/unlabelled cells = 10) at a dye concentration of $10^{-5} \, \text{mol L}^{-1}$. As presented in Figure 5 h, at this dye concentration we could not detect any visual effects of toxicity effects nor impaired cellular growth. Labelled cells divided at the same rate as unlabelled cells and the dye propagated with each division to the daughter cells. In addition, no unspecific spread of the dye from a labelled cell to an adjacent unlabelled cell was observed.

Intracellular Pathway of the WS-TDI Derivatives

For the utilization of the three WS-TDI derivatives it is important to understand their subcellular localization in the endosomal system. Therefore we performed co-localization experiments with cells expressing fusion proteins of the green fluorescent protein with Rab5 or Rab9. Rab proteins belong to the Ras superfamily of small GTPases and are central players of vesicular transport in cells.[26–28] They are especially important to ensure compartment specificity and can be used as compartment markers. Rab5 is a specific GTPase for early endosomes, whereas Rab9 can be used to label late endosomes. HuH7 cells expressing Rab5-GFP or Rab9-GFP were incubated with the three WS-TDI derivatives ($C = 5 \times 10^{-6} \, \text{mol L}^{-1}$). The fluorescence emission of the WS-TDI derivatives and GFP are well separated and allow simultaneous imaging in two separate emission channels using 488 nm and 633 nm laser lines for excitation (for details see Experimental Section). The cells were imaged on a confocal microscope at three different times: i) after

40 min of incubation time with the fluorophore, ii) additional 30 min after washing of the remaining dye and iii) 16 h after washing. Figure 6 shows overlays of the two channels in which
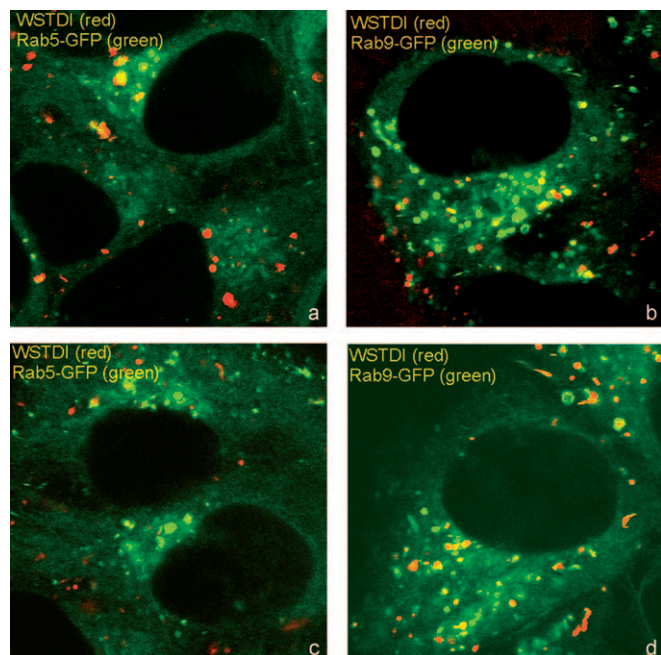

Figure 6. Confocal fluorescence images (71 μm×71 μm) of HuH7 cells expressing Rab5-GFP or Rab9-GFP incubated with WS-TDI. After 40 min incubation, the dye is localized in early (a) as well as late (b) endosomes. Incubation for 60 min followed by 30 min incubation in dye-free medium shows reduced dye-filled early endosomes (c) and pronounced colocalization with late endosomes (d) due to progression of the dye in the endosomal system.

the red color corresponds to the fluorescent signal of the WS-TDI derivatives and the green color to the emission of the GFP Rab GTPases. Direct co-localization of the vesicle containing one of the Rab GTPases and the WS-TDI derivative appears in yellow.

Figures 6a and b show the overlaid fluorescence images of the cells after 40 min of incubation time at 37 °C for WS-TDI dodecyl with the Rab5-GFP and Rab 9-GFP, respectively. At this time the dye can be found in early as well as in late endosomes indicated by the co-localization (yellow signal) of the internalized dye with the Rab5-GFP and Rab9-GFP label in the overlaid images. The non-co-localizing vesicles labelled with WS-TDI (red signal) in Figures 6a and b correspond to other compartments not labelled with GFP. After incubation time of 60 min the cells were washed with PBS in order to remove the excess of the dye in solution. Figures 6c and d show fluorescence images of cells 30 min after washing. In contrast to the images taken with the dye present (and continuously internalized by the cells during image acquisition), nearly no co-localization with early endosomes (marked by Rab5-GFP) can be observed but strong co-localization signals are present with late endosomes (marked by Rab9-GFP). This indicates that the dye has been transferred from early to late endosomes where it remains. Images taken 16 h after washing showed that the dye is still largely localized in late endosomes (data not shown). The

measurements were performed with all three dyes with comparable results (data for other dyes not shown) and confirm that the WS-TDI derivatives can be used as markers for the endocytic system. The dye molecules are first incorporated (within several minutes) in the early endosomes of the cell, then they are progressively transferred to the late endocytic system where the fluorescence signal can be stably observed for several hours. It should be emphasized that the investigation of processes like endosomal transport as well as traffic of other particles within living cells often require very long observation times, especially when processes within a cell cycle have to be observed. Examples are the uptake and transport of viruses[2] and artificial viruses as smart drug-delivery systems[29, 30] in living cells. The utilization of the very photostable WS-TDI derivatives should be of great advantage for such studies.

Virus-Labelling with WS-TDI Pyridoxy

The strong lipophilic nature of the WS-TDI derivatives can also be used to label other types of biological systems like enveloped viruses. In this case, the dye should integrate into the lipid membrane which envelopes the virus. In order to label the viral particles efficiently, it is important that the dye molecule is in a monomeric form as is the case for WS-TDI pyridoxy in water. Therefore we tested the virus labelling properties of this WS-TDI derivative. Herpes simplex type 1 virus particles (HSV1),[31, 32] in which the small capsid protein VP26 has been tagged with GFP were incubated for 1 h with WS-TDI pyridoxy at a concentration of 10^{-6} mol L^{-1}. HSV1 virus particles consist of an icosaedrical capsid surrounded by the tegument and a membrane envelope. However, virus preparations contain intact virus particles as well as capsids without envelope and also empty envelopes[31]. After incubation of a virus preparation with WS-TDI pyridoxy, indeed all three components of the virus preparation were identified as presented in Figures 7a
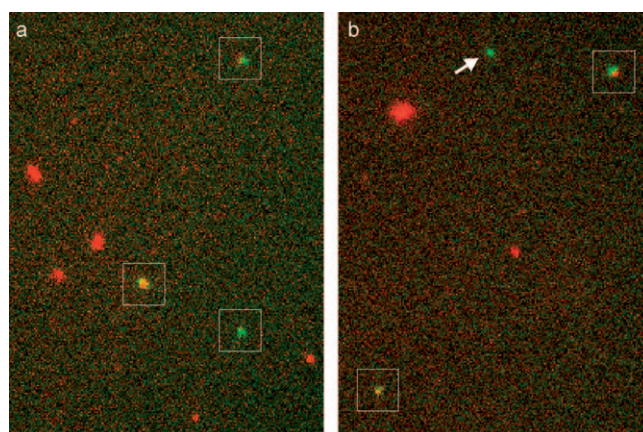

Figure 7. Virus labelling with WS-TDI pyridoxy. HSV1 viral particles with GFP marked capsid (green) were labelled with WS-TDI (red). WS-TDI successfully labelled intact viral particles (see yellow overlap of the particles in the boxes) as well as empty envelopes (red spots). The arrow marks a non-enveloped viral capsid. a) and b) represent different examples of overlaid fluorescence images.

and b. The fluorescence signal of WS-TDI pyridoxy is shown in red whereas viral particles containing GFP-labelled capsids are in green. Co-localization with the WS-TDI pyridoxy signal (yellow particles in the boxes) indicates the successful labelling of enveloped capsids. In addition, unlabelled capsids were found (arrow) suggesting the presence of free capsids without envelope. The structures showing only WS-TDI pyridoxy fluorescence represent TDI-labelled membrane fragments or empty envelopes present in the virus preparation.

These experiments clearly show that with this labelling we can differentiate between intact virus particles and unlabelled capsids as well as membrane fragments. Furthermore, the two color labelling allows following the entry pathway of HSV1 virus particles into living cells in great detail. For example, in the uptake mechanism the viral membrane is fused with the cell membrane. Thus, the capsid can penetrate into the cell cytosol. This process should be observable in the spatial separation of the two colors that is, the WS-TDI pyridoxy identified by its red color is expected to stay in the membrane, and the capsid identified by its green color should move inside the cytosol towards the nucleus. Such experiments are currently being conducted in our group.

2.3. DNA-Labelling with WS-TDI NHS Ester

Another important application is the utilization of WS-TDI for the covalent labelling of specific functional sites in biomolecules. For example, introduction of active amino groups into oligonucleotides such as DNA provides acceptors for a subsequent chemical reaction with the NHS-active ester functionalized WS-TDI. We show here that a single-strand DNA could be successfully labelled with WS-TDI/NHS ester, and that the coupled dye molecule still exhibits a bright fluorescence signal and a high resistance against photobleaching.

In our experiment we used an amino modified DNA oligomer which we reacted with the WS-TDI/NHS ester, as described in the Experimental Section. The labelling efficiency was 30%, which is comparable to efficiencies achieved with commercial dye-labelling kits. The obtained WS-TDI/DNA single strand was subsequently coupled to its complementary strand containing a Biotin tag at one end of the DNA, and an internal ATTO532 label. The resulting double-strand complexes were immobilized at very low concentration to the surface of a cover slip using the Biotin tag, and dual-color fluorescence experiments were performed in order to demonstrate the success of the labelling procedure (see Experimental Section). At the single-molecule level, a double-labelled DNA double strand can be clearly identified by the co-localization of the fluorescence signals of the two spectrally separated fluorophores. The collected fluorescence is divided into two channels corresponding to the spectral regions of the fluorescence of ATTO532/DNA molecules, and WS-TDI/DNA molecules.

Figure 8a shows fluorescence images of a single hybridized DNA molecule obtained from the overlay of the frames before and after 11.2 s of a 300 frames wide-field movie. Since it is highly improbable at such low concentration that two dye molecules occupy by accident the same position, the presence

of a fluorescence spot in both channels demonstrates the success of the DNA labelling as well as of the hybridization procedure. Moreover, after 11.2 s the fluorescence signal of ATTO532/DNA vanishes in a single step, a clear indication of a single molecule. However, such co-localization events of spots arising from single ATTO532/DNA molecules and WS-TDI/DNA occur only for about 10% of the WS-TDI/DNA spots. This is consistent with results obtained by gel electrophoresis (data not shown) which show that aggregation of the WS-TDI molecules still occurs even after the fluorophore has been coupled to the DNA. A large amount of WS-TDI/DNA molecules is trapped in aggregates and is not available for hybridization with complementary ATTO532/DNA strands.

The influence of the DNA strand surrounding the WS-TDI molecule on the photophysical performance of the system can be investigated by evaluating photostability parameters. For this purpose, WS-TDI/DNA molecules were embedded at ultralow concentration ($C \sim 10^{-10}$ mol L^{-1}) in a thin PVA polymer film and fluorescence intensity trajectories of individual molecules were measured and evaluated. Similarly to the study of the new WS-TDI derivatives the probability distributions of TEP and ST were evaluated, and average TEP and ST values were extracted. Additionally, the statistical analysis of the ON and OFF times was performed in order to evaluate the blinking behavior, which is critical for fluorescence resonance energy transfer (FRET) or single-particle tracking studies. For comparison, this procedure was repeated using the same DNA strand but labelled with ATTO647N, a chromophore known for its high performance as a bio-label. The average values of the probability distributions of TEP (left panel), ST (middle panel), and the ON and OFF times (right panel) are shown in Figure 8c. WS-TDI/DNA lives approximately the same time before photobleaching (38 s compared to 34 s) but emits about three times more photons than ATTO647N/DNA (15×10^6 compared to 5.6×10^6). Compared to the performances of the respective free dyes evaluated above, the number of photons emitted by WS-TDI before photobleaching is reduced, whereas the survival time of ATTO647N is increased. However, the comparison of average times of the ON and OFF states shows that WS-TDI/DNA spends significant more time ($14 \times$) in an ON state than ATTO647N/DNA (2.8 s compared to 0.2 s). Moreover, WS-TDI/DNA has a shorter OFF time on average ($2 \times$) than ATTO647N/DNA (0.2 s compared to 0.4 s). These results show that although both attached dye molecules live approximately the same time before photobleaching, WS-TDI/DNA emits many more photons and exhibit much less blinking dynamics. This superior resistance against photodegradation and photoblinking is a crucial advantage for in vivo biological experiments involving marked DNA molecules like in artificial viruses.[30]

3. Conclusions

The photophysical properties of three new water-soluble terrylenediimide dye molecules have been investigated as well as their applications for biological experiments. WS-TDI dodecyl, which results from the addition of an alkyl chain onto WS-TDI, has similar photophysical properties as WS-TDI, and the non-
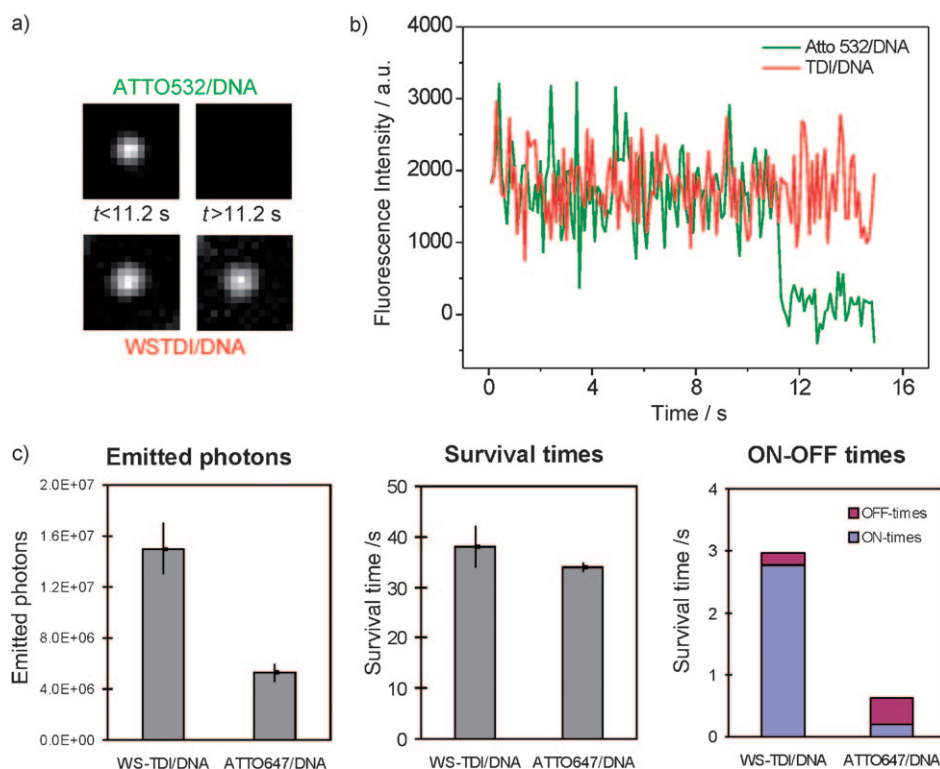
Figure 8. DNA labelling with WS-TDI/NHS ester. a) Averaged fluorescence images showing a single ATTO532/DNA molecule (upper panel) hybridized with its complementary WS-TDI/DNA strand (lower panel) before (left, averaged from 0 to 11.2 s), and after (right, averaged from 11.2 s to the end of the image sequence) the photobleaching event of ATTO532/DNA. The DNA molecules were immobilized using biotin-streptavidin linkers. b) Corresponding fluorescence intensity trajectories for a single ATTO532/DNA and WS-TDI/DNA molecule. c) Averages of total emitted photons (TEP, left panel), Survival times (ST, middle panel), and ON-OFF times (right panel) for WS-TDI/DNA and ATTO647/DNA in PVA polymer films.

fluorescing aggregates in water can be disrupted into fluorescent monomers upon addition of Pluronic or lipid membranes. WS-TDI pyridox, the positively charged form of WS-TDI, forms a new type of chromophore in the WS-TDI family. It is the first analog reported which does not form aggregates and thus fluoresces in water. A single-molecule study revealed that each of these three WS-TDI derivatives exhibits an outstanding photostability compared to other commonly used fluorophores.

The in vivo characterization established that all these WS-TDI derivatives can be used as powerful markers of membranes and membrane-containing compartments of living cells. Indeed, these dyes can be incorporated into early endosomes, and are further transported to late endosomes without being toxic to the cells, and can thus be monitored over several hours.

Due to its more lipophylic nature, WS-TDI dodecyl has the highest affinity for lipid membranes of living cells, and WS-TDI pyridox can successfully stain the envelope of herpes simplex viruses. Finally, it has been shown that a NHS-ester functionalized WS-TDI derivative can be used for the specific labelling of amino groups of a DNA molecule leading to a highly photostable biomolecule.

Experimental Section

New Terrylenediimide Derivatives: The synthesis procedures of WS-TDI dodecyl (N-(2,6-diisopropyl-phenyl)-N′-(n-dodecyl)-1,6,9,14-tetra-(4-sulfonylphenoxy)-terry-lene-3,4:11,12-tetracarboxdiimide) and WS-TDI pyridox (N,N′-(2,6-diisopropylphenyl)-terrylene-1,6,9,14-tetra-(1-methylpyridinium-3yloxy)–3,4:11,12-tetracarboxidi-imide tetramethanesulfonate) are described in detail in the Supporting Information. WS-TDI (1,6,9,14-Tetra(4-sulfonylphenoxy)-N,N′-(2,6-diisopropylphenyl)-terrylene-3,4:11,12-tetracarboxidiimide) and WS-TDI/NHS ester (N-(2,6-diisopropylphenyl)-N′-[5-(N-succinimidyl)-carboxypentyl]-1,6,9,14-tetra(4-sulfonylphenoxy)-terrylene-3,4,11,12-tetracarboxidiimide were synthesized as described previously.[14,16]

UV/Vis Absorption and Fluorescence Spectroscopy: UV/Vis measurements were performed with a Cary 50 Conc spectrophotometer (Varian), and fluorescence spectra measurements with a F900 fluorescence spectrometer (Edinburgh Analytical Instruments). Particle sizes were measured by laser-light scattering using a Malvern Zetasizer 3000HS (Malvern Instruments, Worcestershire, UK). Fluorescence quantum yields were measured by comparing the fluorescence intensity of the sample to that of optically dilute solutions of Cy5 in millipore water ($\Phi_f = 0.27$)[33]. In the quantum yield experiments, changes in the absorption coefficient upon addition of Pluronic P123 (BASF) were compensated for by shifting the excitation wavelength to keep the same total absorption of the sample.

Confocal Microscopy: To investigate the photostability on the single-molecule level, the dye molecules were embedded in polymer matrices. Thin polyvinyl-alcohol (PVA) polymer films (100–200 nm) were prepared by spin-coating polymer solutions in water (2% wt/wt PVA) containing fluorophores with a concentration of 10^{-9} mol L^{-1} for 1 min at 1000 rpm. The dye molecules were excited with a cw He–Ne laser (633 nm) using a modified scanning confocal microscope (ZEISS LSM 410). With this setup, the laser beam was positioned over individual molecules and their fluorescence intensities were recorded as a function of time. The photostability parameters were automatically extracted from the fluorescence time trajectories of individual molecules by custom-written LabView program: i) the number of total emitted photons (TEP) before photobleaching as the integral over a time-trace, ii) the survival time (ST), which is the total duration of the time-trace until photobleaching, and iii) the durations of the ON and OFF times which were selected using a threshold set at a level of two-fold the standard deviation of the mean background signal. From these data we calculated the cumulative probability distributions of the TEP and the ST. These distributions were fitted with a single or bi-exponential decay. From those fits average TEP and average ST were

obtained. Details about the setup and the analysis method can be found elsewhere.[14]

Life-Cell Measurements: HeLa cells (HeLa ACC57, DSMZ, Braunschweig, Germany) were grown in Dulbecco's modified Eagle's medium (DMEM) supplemented with 10% fetal calf serum at 37 °C in 5% CO_2 humidified atmosphere. Cell culture, fetal calf serum and PBS buffer were purchased from Invitrogen GmbH (Karlsruhe, Germany). Dye-uptake experiments were conducted in HeLa cells at 37 °C. For the live-cell imaging experiments solutions of WS-TDI, WS-TDI dodecyl, WS-TDI pyridoxy, and Alexa647/dextran with a concentration of 10^{-5} mol L^{-1} were added to the cells adherent on the surface of a cover-glass. After an incubation time of about 1 h, the solutions were washed out four times with PBS buffer to remove the excess dye.

The fluorescence signal from labelled HeLa cells was monitored either with the confocal microscope described previously or with a wide-field imaging setup. In the latter setup, the dye was excited with a He–Ne lasers at 633 nm. The excitation power was set to 0.2 kW cm^{-2}. This value is far below the saturation intensity of the WS-TDI dyes, which is about 1 MW cm^{-2} as measured by fluorescence correlation spectroscopy (unpublished data). The laser beam was expanded and focused onto the back-focal plane of a microscope objective (Nikon Plan Apo 100x/1.4 oil inside a Nikon eclipse TE200 microscope). Fluorescence was collected by the same objective, separated from backscattered laser light with a combination of filters (dichroic mirror 640 nm cutoff and band-pass BP730/140 AHF) and imaged onto a back-illuminated CCD detector (Andor, iXon DV897). Movie 1 (see Supporting Information) was recorded with magnification corresponding to 122 nm per pixel and an integration time of 500 ms per frame.

Subcellular Localization of the Three WS-TDI Derivatives: HuH7 cells (JCRB 0403; Tokyo, Japan) were grown in DMEM:F12 (1:1) with Glutamax I medium supplemented with 10% FCS at 37 °C in 5% CO2 humidified atmosphere. For wide-field microscopy, cells were plated on collagen-A-coated LabTek chambered cover glass (Nunc, Rochester, USA) 24 to 48 h before imaging. Cells were imaged in CO_2-independent medium (Invitrogen) on a heated microscope stage at 37 °C. To generate HuH7 cells stably expressing Rab5-GFP and Rab9-GFP, cells were transfected using Lipofectamine (Invitrogen) and subsequently selected with G418 (0.6 mg mL^{-1}). Fluorescence signal was monitored with a commercial confocal microscope (LSM 510) using a 488 nm laser.

Long-Term Toxicity Assays: HeLa cells were incubated with a solution of WS-TDI (C = 10^{-5} mol L^{-1}) for 1 h in the incubator. After the incubation period, the labelled cells were washed with PBS and trypsinized. The labelled cells were mixed with unlabelled cells in a ratio labelled/unlabelled cells = 10 and plated on a 35 mm glass bottom Petri dish/LabTek chambered cover glass (Ibidi, Martinsried, Germany) at a cell density of 10^4 cells per well. Cellular growth and dye distribution within the cells was monitored by imaging the same region of the Petri dish for three subsequent days in 8–12 h intervals.

Virus Labelling with WS-TDI Pyridoxy: In order to label viral envelopes, virus particles were incubated with 1 µg mL^{-1} WS-TDI pyridoxy for two hours at room temperature. To remove unbound dye, virus particles were dialysed on a 0.025 µm pore diameter nitrocellulose membrane (Millipore) against buffer containing 50 mM HEPES, 145 mM NaCl, 0.2% (w/v) BSA, pH 7.3 and imaged on a wide-field set-up. The fluorophores were excited with a 488 nm laser for GFP, and a 633 nm laser for WS-TDI.

Synthesis of TDI-Labelled Oligonucleotides: WS-TDI was covalently attached to a single-stranded oligonucleotide (70 bases, (5')-A AGA GAG TGA GGA CGA ACG CGC CCC CAC CCC CTT TTA TAG CCC **T**CC TCC AGG AAC ACC CGG TCA CGT GGC, IBA, Germany) at position 44 (Thymin in bold) via a 6-carbon atom amino linker using an NHS derivative. One equivalent of oligonucleotide was incubated with a seven-fold excess of dye in sodium tetraborate buffer (pH 8.5) at 50 °C for one hour. Labelled oligonucleotide was then precipitated in ethanol, leaving non-aggregated WS-TDI in solution. After re-suspending in phosphate buffered saline (PBS) the oligonucleotide was further purified using size exclusion chromatography (Biorad P-6) according to manufacturer's instructions. The labelled oligonucleotide was then hybridized to its complementary strand (using 5-fold excess of WS-TDI/DNA) containing Biotin on its 3'-end for later immobilization. For further colocalisation an ATTO532 dye molecule was attached at position 44 on the complementary strand.

Single-molecule experiments were performed on a custom-built prism-based total internal reflection fluorescence microscope (TIRFM). Details about the experimental setup can be found elsewhere.[23, 34] The sample is excited alternately using both a frequency-doubled Nd–YAG laser (Spectra Physics) at 532 nm for the excitation of ATTO532 molecules and a Diode-laser (Coherent) at 637 nm for excitation of WS-TDI molecules. A 30 nm bandpass filter at 580 nm and a 75 nm bandpass filter at 760 nm were used in the spectrally separated detection paths. Fluorescence light was imaged using an EM-CCD (Andor).

Acknowledgements

[1] J. Lippincott-Schwartz, E. Snapp, A. Kenworthy, *Nat. Rev.* **2001**, *2*, 444–456.
[2] G. Seisenberger, M. U. Ried, T. Endreß, H. Büning, M. Hallek, C. Bräuchle, *Science* **2001**, *294*, 1929–1932.
[3] R. Roy, S. Hohng, T. Ha, *Nat. Methods* **2008**, *5*, 507–516.
[4] C. Joo, H. Balci, Y. Ishitsuka, C. Buranachai, T. Ha, *Annu. Rev. Biochem.* **2008**, *77*, 51–76.
[5] S. A. Kim, K. G. Heinze, M. N. Waxham, P. Schwille, *Proc. Natl. Acad. Sci. USA* **2004**, *101*, 105–110.
[6] A. Yildiz, J. N. Forkey, S. A. McKinney, T. Ha, Y. E. Goldman, P. R. Selvin, *Science* **2003**, *300*, 2061–2065.
[7] S. Weiss, *Nat. Struct. Bio.* **2000**, *7*, 724–729.
[8] S. Weiss, *Science* **1999**, *283*, 1676–1683.
[9] E. J. G. Peterman, H. Sosa, W. E. Moerner, *Annu. Rev. Phys. Chem.* **2004**, *55*, 79–96.
[10] E. J. G. Peterman, H. Sosa, L. S. B. Goldstein, W. E. Moerner, *Biophys. J.* **2001**, *81*, 2851–2863.
[11] S. A. Kim, K. G. Heinze, P. Schwille, *Nat. Methods* **2007**, *4*, 963–973.
[12] J. Elf, G. W. Li, X. S. Xie, *Science* **2007**, *316*, 1191–1194.

[13] A. Dubois, M. Canva, A. Brun, F. Chaput, J. P. Boilot, *Appl. Opt.* **1996**, *35*, 3193–3199.

[14] C. Jung, B. K. Muller, D. C. Lamb, F. Nolde, K. Mullen, C. Brauchle, *J. Am. Chem. Soc.* **2006**, *128*, 5283–5291.

[15] J. Q. Fabian Nolde, Christopher Kohl, Neil G. Pschirer, Erik Reuther, Klaus Müllen„ *Chem.-Eur. J.* **2005**, *11*, 3959–3967.

[16] K. Peneva, G. Mihov, F. Nolde, S. Rocha, J. Hotta, K. Braeckmans, J. Hofkens, H. Uji-I, A. Herrmann, K. Mullen, *Angew. Chem.* **2008**, *120*, 3420–3423; *Angew. Chem. Int. Ed.* **2008**, *47*, 3372–3375.

[17] S. Das, K. G. Thomas, K. J. Thomas, V. Madhavan, D. Liu, P. V. Kamat, M. V. George, *J. Phys. Chem.* **1996**, *100*, 17310–17315.

[18] A. Czimerova, J. Bujdak, A. Gaplovsky, *Colloids Surf. A* **2004**, 243, 89–96.

[19] M. Kasha, H. R. Rawls, M. A. El-Bayoumi, *Pure Appl. Chem.* **1965**, *11*, 371–392.

[20] E. G. McRae, M. Kasha, *J. Chem. Phys.* **1958**, *28*, 721–722.

[21] S. B. Brichkin, M. A. Kurandina, T. M. Nikolaeva, V. F. Razumov, *High Energy Chem.* **2004**, *38*, 373–380.

[22] A. N. Kapanidis, E. Margeat, S. O. Ho, E. Kortkhonjia, S. Weiss, R. H. Ebright, *Science* **2006**, *314*, 1144–1147.

[23] J. Andrecka, R. Lewis, F. Bräckner, E. Lehmann, P. Cramer, J. Michaelis, *Proc. Natl. Acad. Sci. USA* **2008**, *105*, 135–140.

[24] M. M. Lampton, Bruce & Bowyer, Stuart, *Astrophys. J.* **1976**, *208,* 177–190.

[25] N. Bobroff, *Rev. Sci. Instrum.* **1986**, *57,* 1152–1157.

[26] B. L. Grosshans, D. Ortiz, P. Novick, *Proc. Natl. Acad. Sci. USA* **2006**, 103, 11 821–11 827.

[27] K. Mohrmann, P. van der Sluijs, *Mol. Membr. Biol.* **1999**, *16*, 81–87.

[28] M. R. G. Russell, D. P. Nickerson, G. Odorizzi, *Curr. Opin. Cell Bio.* **2006**, *18*, 422–428.

[29] R. Bausinger, K. Von Gersdorff, K. Braeckmans, M. Ogris, E. Wagner, C. Bräuchle, A. Zumbusch, *Angew. Chem.* **2006**, *118*, 1598–1602; *Angew. Chem. Int. Ed.* **2006**, *45*, 1568–1572.

[30] K. de Bruin, N. Ruthardt, K. von Gersdorff, R. Bausinger, E. Wagner, M. Ogris, C. Bräuchle, *Mol. Ther.* **2007**, *15*, 1297–1305.

[31] K. Dohner, K. Radtke, S. Schmidt, B. Sodeik, *J. Virol.* **2006**, *80*, 8211–8224.

[32] C. H. Nagel, K. Dohner, M. Fathollahy, T. Strive, E. M. Borst, M. Messerle, B. Sodeik, *J. Virol.* **2008**, *82*, 3109–3124.

[33] R. B. Mujumdar, L. A. Ernst, S. R. Mujumdar, C. J. Lewis, A. S. Waggoner, *Bioconj. Chem.* **1993**, *4*, 105–111.

[34] R. Lewis, H. Durr, K. P. Hopfner, J. Michaelis, *Nucleic Acids Res.* **2008**, *36*, 1881–1890.